Zernike expansions for non-Kolmogorov turbulence

Glenn D. Boreman

Center for Research and Education in Optics and Lasers, Department of Electrical Engineering, University of Central Florida, Orlando, Florida 32816

Christopher Dainty

Blackett Laboratory, Imperial College, London SW7 2BZ, United Kingdom

Received June 19, 1995; revised manuscript received August 21, 1995; accepted September 12, 1995

We investigate the expression of non-Kolmogorov turbulence in terms of Zernike polynomials. Increasing the power-law exponent of the three-dimensional phase power spectrum from 2 to 4 results in a higher proportion of wave-front energy being contained in the tilt components. Closed-form expressions are given for the variances of the Zernike coefficients in this range. For exponents greater than 4 a von Kármán spectrum is used to compute the variances numerically as a function of exponent for different outer-scale lengths. We find in this range that the Zernike-coefficient variances depend more strongly on outer scale than on exponent and that longer outer-scale lengths lead to more energy in the tilt terms. The scaling of Zernike-coefficient variances with pupil diameter is an explicit function of the exponent.

Key words: atmospheric turbulence, Zernike polynomials, non-Kolmogorov, adaptive optics.

1. INTRODUCTION

Although the Kolmogorov formulation[1] has been widely used to describe atmospheric turbulence, some turbulence conditions exist for which experimental data do not support it. For Kolmogorov turbulence the three-dimensional power spectral density of phase fluctuations has the form

$$\Phi_\varphi(k) = \frac{0.023\,k^{-11/3}}{r_0{}^{5/3}}, \tag{1}$$

where k is spatial frequency (cycles/length) and r_0 is a normalization factor with units of length that gives the correct dimensionality of the power spectrum.[2] We interpret r_0 as the pupil diameter over which the piston-subtracted wave-front variance is equal to 1 rad^2 for the case of Kolmogorov turbulence. We find this definition more convenient for our purposes than the original[3] definition of r_0 in terms of the integral of the modulation transfer function. These two definitions agree to within a few percent.

The exponent for the inverse spatial-frequency dependence has been observed experimentally to be both larger and smaller than the value of 11/3 that derives from the Kolmogorov theory. Exponent values near 5 are encountered in high-altitude (stratospheric) stellar-scintillation studies,[4,5] while measurements affected by turbulence nearer to the ground[6–8] yield exponents in the range of 3 to 3.65. It is thus of interest to investigate the behavior of non-Kolmogorov turbulence[9–11] having a range of exponents.

An alternative definition exists in the literature for the term non-Kolmogorov turbulence, which is that outer-scale effects are included for the case in which the power-law exponent is assumed to be 11/3. The derivation of Zernike-variance coefficients in this context has been explored in detail by Winker.[12] In the present paper we perform a wave-front expansion for the general-exponent case in terms of variances of Zernike coefficients and include outer-scale effects for the range of exponents where they are required for evaluation of the expressions. This is useful in determining the relative amounts of tilt and other low-order aberrations in the turbulent wave front as well as in analysis of experimental data from Shack–Hartmann wave-front sensors.[13]

The generalized form of Eq. (1) for the phase spectrum is

$$\Phi_\varphi(k) = \frac{A_\beta k^{-\beta}}{\aleph_0^{\beta-2}}, \tag{2}$$

where $\aleph_0$ is a quantity analogous to r_0 that reduces to r_0 for the case of $\beta = 11/3$. The constant A_β has a value such that, for any power law β chosen for the spectrum, the piston-subtracted wave-front variance (which we denote Δ_1) is normalized to 1 rad^2 over a pupil diameter $D = \aleph_0$. The numerical values of the Zernike-coefficient variances (which we denote $\langle|a_j{}^2|\rangle$) are then the relative wave-front energies contained in each Zernike term. Because the wave-front variance directly affects image quality, this normalization provides an equivalent-image-quality basis for comparison of the amounts of the different aberrations in the turbulent wave front as a function of β.

To verify that the parameter $\aleph_0$ ensures correct dimensionality in the phase spectrum, we express the phase structure function $D_\varphi(r)$ as

$$D_\varphi(r) \propto 2\int |\bar{k}|^{-\beta}\{1 - \exp[i2\pi(\bar{k}\cdot\bar{r})]\}\mathrm{d}\bar{k}. \tag{3}$$

Given that

$$\int \mathrm{d}\bar{k} \equiv \int_0^{2\pi} \mathrm{d}\phi \int_0^{\infty} k\,\mathrm{d}k, \tag{4}$$

0740-3232/96/030517-06$06.00

Table 1. Correspondence between j, n, m, and the Lowest-Order Aberrations

Mode Number j	Radial Degree n	Azimuthal Frequency m
1 (piston)	0	0
2 (x tilt)	1	1
3 (y tilt)	1	1
4 (defocus)	2	0
5	2	2
6 (astigmatism)	2	2
7 (x coma)	3	1
8 (y coma)	3	1
9	3	3
10	3	3
11 (spherical)	4	0

we find, upon performing the integration in Eq. (3), that $D_\varphi(r)$ is proportional to $r^{\beta-2}$. Thus, because we desire to express the structure function (and ultimately the Zernike-coefficient variances) in terms of a normalized pupil diameter (D/r_0), the form of the phase spectrum must be as shown in Eq. (2), with a term of $r_0^{\beta-2}$ in the denominator.

2. ZERNIKE EXPANSION AND RESIDUAL WAVE-FRONT ERROR

We use the definitions of Noll[14] for the Zernike polynomials and their Fourier transforms. We perform all calculations with the transform-domain Zernike polynomials,

$$Q_j(k,\phi) = \sqrt{n+1}\,\frac{J_{n+1}(2\pi k)}{\pi k} \times \begin{cases} (-1)^{n/2}\sqrt{2}\cos m\phi, & j \text{ even} \\ (-1)^{n/2}\sqrt{2}\sin m\phi, & j \text{ odd} \\ (-1)^{n/2}, & m = 0 \end{cases}, \tag{5}$$

where ϕ is the azimuthal angle in the transform domain, j is the mode number, n is the radial degree, and m is the azimuthal frequency. These numbers[15] correspond to the first few classical aberrations seen in Table 1, suitable for analysis of a low-order-correction adaptive-optical system.

We are interested in the residual mean-squared wave-front error Δ_J after terms from $j = 1$ to J are corrected (as with an adaptive-optical system), defined as

$$\Delta_J = \langle \varphi^2 \rangle - \sum_{j=1}^{J} \langle |a_j|^2 \rangle, \tag{6}$$

where $\langle \varphi^2 \rangle$ is the total phase variance of the random wave front,

$$\langle \varphi^2 \rangle = \sum_{j=1}^{\infty} \langle |a_j|^2 \rangle, \tag{7}$$

and the $\langle |a_j|^2 \rangle$ are the Zernike-coefficient variances. The piston variance $\langle |a_1|^2 \rangle$ is infinite, and the phase variance is also infinite if outer-scale effects are neglected. These infinities cancel when the two terms are subtracted. The resulting piston-subtracted wave-front variance Δ_1 is normalized to 1:

$$\Delta_1 = \langle \varphi^2 \rangle - \langle |a_1|^2 \rangle = \sum_{j=2}^{\infty} \langle |a_j|^2 \rangle = 1, \tag{8}$$

which determines the value of A_β (Appendix A).

The Zernike-coefficient variances are defined[14] as

$$\langle |a_j{}^2| \rangle = \int_{-\infty}^{\infty} \int_{-\infty}^{\infty} Q_j{}^*(k) Q_j(k') \Phi_\varphi(k/R, k'/R) \mathrm{d}\bar{k}\, \mathrm{d}\bar{k}', \tag{9}$$

where R is the pupil radius, and the general form of the cross-phase spectrum is

$$\Phi_\varphi(k/R, k'/R) = A_\beta \left(\frac{R}{r_0}\right)^{\beta-2} k^{-\beta} \delta(k - k'). \tag{10}$$

If we substitute Eq. (10) into Eq. (9), the expression for the Zernike-coefficient variances becomes

$$\langle |a_j|^2 \rangle = A_\beta \left(\frac{R}{r_0}\right)^{\beta-2} \int_{-\infty}^{\infty} \int_{-\infty}^{\infty} Q_j{}^* Q_j k^{-\beta} \delta(k - k') \mathrm{d}\bar{k}\, \mathrm{d}\bar{k}'. \tag{11}$$

Using Eqs. (4) and (5), we can write Eq. (11) as

$$\langle |a_j|^2 \rangle = \frac{2A_\beta}{\pi} \left(\frac{R}{r_0}\right)^{\beta-2} (n+1) \int_0^{\infty} k^{-(\beta+1)} J_{n+1}^2(2\pi k) \mathrm{d}k, \tag{12}$$

which is valid for any m, and for any n not equal to zero. Performing a change of variables, $2\pi k = \kappa$, we obtain

$$\langle |a_j|^2 \rangle = \frac{2A_\beta}{\pi} \left(\frac{R}{r_0}\right)^{\beta-2} (n+1)(2\pi)^{\beta} \int_0^{\infty} \kappa^{-(\beta+1)} J_{n+1}^2(\kappa) \mathrm{d}\kappa. \tag{13}$$

Using $2R = D$, we find that the Zernike-coefficient variances have a $(D/r_0)^{\beta-2}$ dependence:

$$\langle |a_j|^2 \rangle = 8A_\beta \left(\frac{D}{r_0}\right)^{\beta-2} (n+1)\pi^{\beta-1} \int_0^{\infty} \kappa^{-(\beta+1)} J_{n+1}^2(\kappa) \mathrm{d}\kappa. \tag{14}$$

It should be noted that the scaling of the Zernike-coefficient variances with pupil diameter is explicitly a function of β.

The integral in Eq. (14) can be expressed in closed form[16] as

$$\int_0^{\infty} \kappa^{-(\beta+1)} J_{n+1}^2(\kappa) \mathrm{d}\kappa = \frac{\Gamma(\beta+1)\Gamma\left(\frac{2n+2-\beta}{2}\right)}{2^{\beta+1}\left[\Gamma\left(\frac{\beta+2}{2}\right)\right]^2 \Gamma\left(\frac{2n+4+\beta}{2}\right)} \tag{15}$$

for β and n satisfying $(2n+2) > \beta > -1$. In that range the Zernike-coefficient variances are expressed as

$$\langle |a_j|^2 \rangle = 8A_\beta \left(\frac{D}{r_0}\right)^{\beta-2} (n+1)\pi^{\beta-1} \times \frac{\Gamma(\beta+1)\Gamma\left(\frac{2n+2-\beta}{2}\right)}{2^{\beta+1}\left[\Gamma\left(\frac{\beta+2}{2}\right)\right]^2 \Gamma\left(\frac{2n+4+\beta}{2}\right)}. \tag{16}$$

For the piston case ($j = 1$, $n = 0$) the integral of Eq. (15) diverges for $\beta > 2$, which includes all cases of interest to

Table 2. Comparison of $\langle|a_j|^2\rangle$ for $\beta = 11/3$ and $D = r_0$ Calculated with Eq. (17) to Those of Ref. 12

$\langle\|a_j\|^2\rangle$	From Eq. (17)	From Ref. 12
$\langle\|a_{2-3}\|^2\rangle$	0.434783	0.4479
$\langle\|a_{4-6}\|^2\rangle$	0.022489	0.0232
$\langle\|a_{7-10}\|^2\rangle$	0.005997	0.0062
$\langle\|a_{11}\|^2\rangle$	0.002377	0.0024

us. We will see below that $\beta = 2$ corresponds to the case in which the wave-front variance is entirely contained in the piston term.

Using the normalization condition of Eq. (8), we develop an expression for A_β in Appendix A as Eq. (A13). Combining Eqs. (16) and (A13), we find that

$$\langle|a_j|^2\rangle = \left(\frac{D}{r_0}\right)^{\beta-2}\frac{(n+1)}{\pi} \times \frac{\Gamma\left(\frac{2n+2-\beta}{2}\right)\Gamma\left(\frac{\beta+4}{2}\right)\Gamma\left(\frac{\beta}{2}\right)\sin\left(\pi\frac{\beta-2}{2}\right)}{\Gamma\left(\frac{2n+4+\beta}{2}\right)}. \tag{17}$$

Equation (17) is valid for $n \geq 1$ and $2 < \beta < 4$. Referring to Eq. (17) and Table 1, we see that the Zernike-coefficient variances are equal for any j having the same value of n. We use the notation

$$\langle|a_{2-3}|^2\rangle \equiv \langle|a_2|^2\rangle = \langle|a_3|^2\rangle, \tag{18}$$

$$\langle|a_{4-6}|^2\rangle \equiv \langle|a_4|^2\rangle = \langle|a_5|^2\rangle = \langle|a_6|^2\rangle, \tag{19}$$

$$\langle|a_{7-10}|^2\rangle \equiv \langle|a_7|^2\rangle = \langle|a_8|^2\rangle = \langle|a_9|^2\rangle = \langle|a_{10}|^2\rangle. \tag{20}$$

To facilitate comparison with the work of Fried[2] and Noll,[14] considering our slightly different definition of r_0, we give the first few $\langle|a_j|^2\rangle$ terms calculated with Eq. (17) for the Kolmogorov case of $\beta = 11/3$ and find good agreement with previously published values, as shown in Table 2.

3. ZERNIKE-VARIANCE COEFFICIENTS FOR $2 < \beta < 4$

We evaluate Eq. (17) with $2 \leq j \leq 11$ and $2 < \beta < 4$ for the case of $D = r_0$. The Zernike-coefficient variances scale with pupil diameter as $(D/r_0)^{\beta-2}$, consistent with Eq. (17). Figure 1 shows the two tilt terms $\langle|a_{2-3}|^2\rangle$ as a function of β, and Fig. 2 shows three curves for the next-higher-order terms: $\langle|a_{4-6}|^2\rangle$, $\langle|a_{7-10}|^2\rangle$, and $\langle|a_{11}|^2\rangle$, as functions of β.

All of the variances obey the normalization condition expressed in Eq. (8) for any given value of β, and thus the sum over all the coefficients for $j \geq 2$ must be unity. All of the coefficients approach zero as β approaches 2. Equation (3) shows that for $\beta = 2$ the structure function $D_\varphi(r)$ would be a constant, depending on the zeroth power of separation distance. This corresponds to the case in which the phase variance is contained solely in the piston term. Thus we consider only the case of $\beta > 2$ as having physical significance. Because the set of Zernike-coefficient variances is normalized, more terms are required (as the terms themselves get smaller) for an accurate representation of the wave front as β approaches 2. This shift of the wave-front energy to higher orders is consistent with decreasing the tilt components, under the normalization condition of $\Delta_1 = 1$. As shown in Fig. 3, as n increases, the terms decrease in magnitude, but each successive term peaks at a lower value of β and is progressively skewed to have its main contribution for smaller β. This increases the relative importance of the higher-order terms as β approaches 2.

As β increases toward 4, the two tilt coefficients of Fig. (1) increase toward 0.5. Although Eq. (17) has a singularity at $\beta = 4$, the interpretation is that an increasing amount of the energy in the piston-subtracted wave

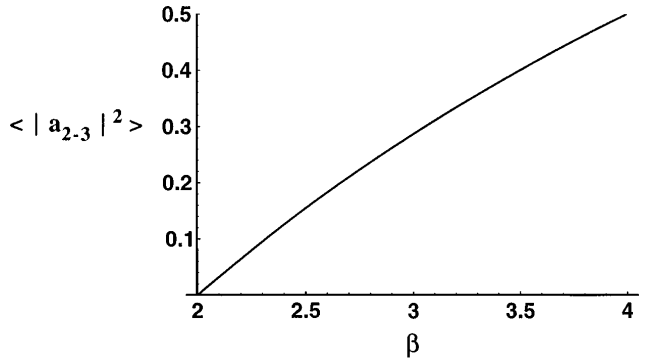

Fig. 1. Zernike-tilt-coefficient variances (for the case of $D = r_0$) $\langle|a_{2-3}|^2\rangle$ as a function of β, for $2 < \beta < 4$.

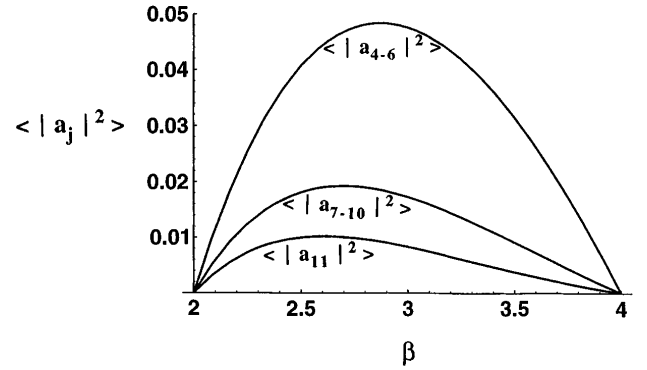

Fig. 2. Higher-order Zernike-coefficient variances (for the case of $D = r_0$) $\langle|a_{4-6}|^2\rangle$, $\langle|a_{7-10}|^2\rangle$, and $\langle|a_{11}|^2\rangle$, as functions of β, for $2 < \beta < 4$.

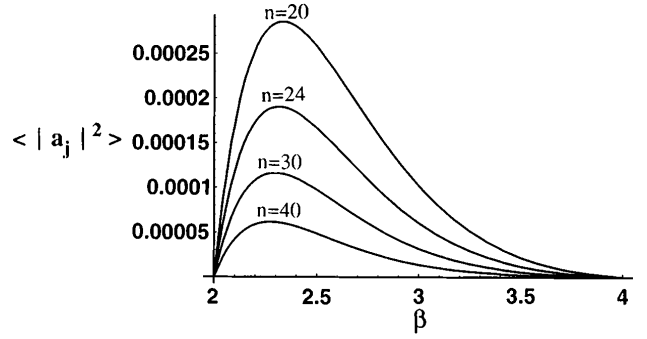

Fig. 3. Zernike-coefficient variances peak at lower values of β, as n increases. Plots are for $\langle|a_j|^2\rangle$ (for the case of $D = r_0$) corresponding to $n = 20$, 24, 30, and 40.

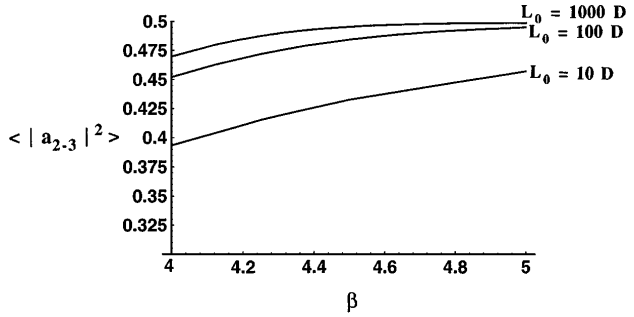

Fig. 4. Zernike-tilt-coefficient variances (for the case of $D = r_0$) $\langle |a_{2-3}|^2 \rangle$ as a function of β, for $\beta > 4$, with $L_0/D = 10$, 100, and 1000.

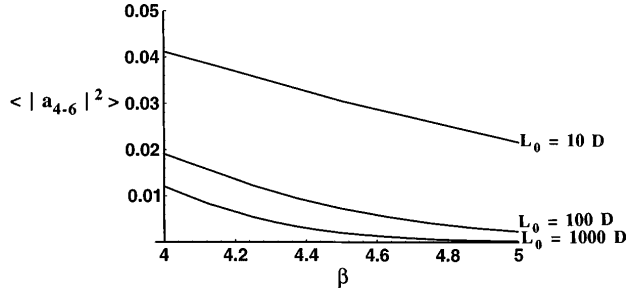

Fig. 5. Zernike-coefficient variances (for the case of $D = r_0$) $\langle |a_{4-6}|^2 \rangle$ as a function of β, for $\beta > 4$, with $L_0/D = 10$, 100, and 1000.

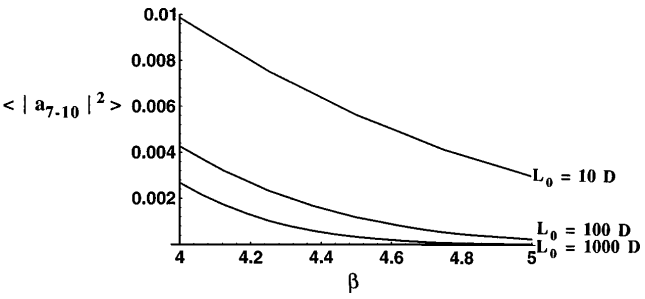

Fig. 6. Zernike-coefficient variances (for the case of $D = r_0$) $\langle |a_{7-10}|^2 \rangle$ as a function of β, for $\beta > 4$, with $L_0/D = 10$, 100, and 1000.

front are contained in the tilt terms as β approaches 4. Figures 2 and 3 show that all of the coefficients for $j > 3$ approach zero as β approaches 4, as required by the normalization, because an increasing amount of energy is contained in the tilt terms.

Figures 1 and 2 [or Eq. (17)] can be used to evaluate the residual mean-squared error Δ_J according to Eqs. (6) and (8) for any $4 > \beta > 2$.

4. ZERNIKE-VARIANCE COEFFICIENTS FOR $\beta > 4$

Equation (17) for the Zernike-coefficient variances is not valid in the range $\beta > 4$, so we use numerical techniques to investigate the variances as a function of β for different outer-scale lengths. Combining Eqs. (14) and (A10) yields an expression for the Zernike-coefficient variances in terms of spatial-frequency integrals:

$$\langle |a_j|^2 \rangle = 4(n+1)\left(\frac{D}{r_0}\right)^{\beta-2} \frac{\int_0^\infty \kappa^{-(\beta+1)} J_{n+1}^2(\kappa)\,\mathrm{d}\kappa}{\int_0^\infty \kappa^{-(\beta-1)}\left\{1 - \frac{4J_1^2(\kappa)}{\kappa^2}\right\}\mathrm{d}\kappa}. \tag{21}$$

The integrals involved in Eq. (21) are divergent for small κ. In order to examine the effect of the power-law exponent β on the Zernike-coefficient variances, we must include an outer-scale dimension in the calculation. We used the von Kármán[1] spectrum as a convenient means to accomplish this. Qualitatively similar results should be obtained by use of alternative outer-scale expressions,[17] such as the Greenwood or exponential models. Modifying Eq. (2) in this way yields

$$\Phi_\varphi(k) = \frac{A_\beta\left[k^2 + \left(\frac{R}{L_0}\right)^2\right]^{-\beta/2}}{r_0{}^{\beta-2}}. \tag{22}$$

We express Eq. (22) in terms of $\kappa = 2\pi k$ to yield

$$\Phi_\varphi(\kappa) = \frac{A_\beta\left[\kappa^2 + \left(2\pi\frac{R}{L_0}\right)^2\right]^{-\beta/2}}{r_0{}^{\beta-2}}. \tag{23}$$

Substituting $D = 2R$ yields

$$\Phi_\varphi(\kappa) = \frac{A_\beta\left[\kappa^2 + \left(\pi\frac{D}{L_0}\right)^2\right]^{-\beta/2}}{r_0{}^{\beta-2}}. \tag{24}$$

If Eq. (24) is used in a development similar to that which produced Eq. (21), the analogous expression is

$$\langle |a_j|^2 \rangle = 4(n+1)\left(\frac{D}{r_0}\right)^{\beta-2} \times \frac{\int_0^\infty \left[\kappa^2 + \left(\pi\frac{D}{L_0}\right)^2\right]^{-\beta/2} \kappa^{-1} J_{n+1}^2(\kappa)\,\mathrm{d}\kappa}{\int_0^\infty \left[\kappa^2 + \left(\pi\frac{D}{L_0}\right)^2\right]^{-\beta/2} \kappa\left(1 - \frac{4J_1^2(\kappa)}{\kappa^2}\right)\mathrm{d}\kappa}. \tag{25}$$

We choose the following outer scales for the computation of the $\langle |a_j|^2 \rangle$ from Eq. (25): $L_0 = 10D$, $L_0 = 100D$, and $L_0 = 1000D$. Figure 4 shows $\langle |a_{2-3}|^2 \rangle$, Fig. 5 shows $\langle |a_{4-6}|^2 \rangle$, and Fig. 6 shows $\langle |a_{7-10}|^2 \rangle$, all as functions of β and L_0/D, for the case of $D = r_0$.

We note from Figs. 4–6 that the coefficients have a stronger dependence on L_0 than on β. For any given β, a decreasing outer scale takes energy away from the tilt terms. The normalization of Eq. (8) then requires that the higher-order terms gain energy as L_0 decreases. Conversely, the tilt terms dominate the expansion for large L_0. Also, increased values of β lead to larger amounts of tilt.

5. CONCLUSIONS

We investigated the behavior of the Zernike-coefficient variances of a turbulent wave front having a general exponent β. Our normalization of unity piston-subtracted

wave-front variance provides an equal-image-quality comparison of the relative energy content of the various Zernike components in the turbulent wave front as β varies. The scaling of the Zernike-coefficient variances with pupil diameter is proportional to $(D/r_0)^{\beta-2}$.

For $2 < \beta < 4$, the amount of energy in the tilt terms increases nearly linearly with β, with the limit that the tilt terms contain all of the energy at $\beta \to 4$. The higher-order terms increase in importance for smaller values of β. The case of $\beta = 2$ corresponds to the case in which all of the variance of the turbulent wave front is contained in the piston term.

For $\beta > 4$, an outer scale L_0 must be assumed in the calculation. The tilt terms dominate the expansion with increasing outer scale or increasing β. The higher-order terms correspondingly decrease with increasing L_0 and β. Consistent with Ref. 9, the Zernike-coefficient variances show a stronger dependence on L_0 than on β, for $\beta > 4$.

APPENDIX A: CALCULATION OF A_β

We develop an expression for Δ_1, which will be solved for A_β. The resulting expression for A_β will be used in Eq. (16) for the Zernike-coefficient variances. We express the phase variance as[12]

$$\langle \varphi^2 \rangle = 2\pi \int_0^\infty k \Phi_\varphi(k/R) \mathrm{d}k , \tag{A1}$$

and, upon substituting Eq. (10), we obtain

$$\langle \varphi^2 \rangle = 2\pi A_\beta \left(\frac{R}{r_0} \right)^{\beta-2} \int_0^\infty k^{-(\beta-1)} \mathrm{d}k , \tag{A2}$$

$$\langle \varphi^2 \rangle = \pi A_\beta \left(\frac{D}{r_0} \right)^{\beta-2} 2^{-(\beta-3)} \int_0^\infty k^{-(\beta-1)} \mathrm{d}k . \tag{A3}$$

To combine Eq. (A3) with Eq. (14), we make the same change of variables $2\pi k = \kappa$, to yield

$$\langle \varphi^2 \rangle = \pi A_\beta \left(\frac{D}{r_0} \right)^{\beta-2} 2^{-(\beta-3)} \int_0^\infty \left(\frac{\kappa}{2\pi} \right)^{-(\beta-1)} \frac{\mathrm{d}\kappa}{2\pi} , \tag{A4}$$

$$\langle \varphi^2 \rangle = \pi A_\beta \left(\frac{D}{r_0} \right)^{\beta-2} 2^{-(\beta-3)} (2\pi)^{(\beta-2)} \int_0^\infty \kappa^{-(\beta-1)} \mathrm{d}\kappa , \tag{A5}$$

$$\langle \varphi^2 \rangle = A_\beta \left(\frac{D}{r_0} \right)^{\beta-2} 2\pi^{\beta-1} \int_0^\infty \kappa^{-(\beta-1)} \mathrm{d}\kappa . \tag{A6}$$

Substituting Eq. (14) (for the case of $j = 1$, $n = 0$) and Eq. (A6) into Eq. (8) yields

$$\begin{aligned} \Delta_1 &= \langle \varphi^2 \rangle - \langle |a_1|^2 \rangle \\ &= 2A_\beta \left(\frac{D}{r_0} \right)^{\beta-2} \pi^{\beta-1} \int_0^\infty \kappa^{-(\beta-1)} \mathrm{d}\kappa \\ &\quad - 8A_\beta \left(\frac{D}{r_0} \right)^{\beta-2} \pi^{\beta-1} \int_0^\infty \kappa^{-(\beta+1)} J_1^{\,2}(\kappa) \mathrm{d}\kappa , \end{aligned} \tag{A7}$$

$$\Delta_1 = \pi^{\beta-1} 2A_\beta \left(\frac{D}{r_0} \right)^{\beta-2} \left\{ \int_0^\infty \kappa^{-(\beta-1)} - 4[\kappa^{-(\beta+1)} J_1^{\,2}(\kappa)] \mathrm{d}\kappa \right\} , \tag{A8}$$

$$\Delta_1 = \pi^{\beta-1} 2A_\beta \left(\frac{D}{r_0} \right)^{\beta-2} \left(\int_0^\infty \kappa^{-(\beta-1)} \left\{ 1 - 4 \left[\frac{J_1^{\,2}(\kappa)}{\kappa^2} \right] \right\} \mathrm{d}\kappa \right) . \tag{A9}$$

With the normalization of $\Delta_1 = 1$ at $D = r_0$, we have

$$A_\beta = 1 \Big/ \left\{ 2\pi^{\beta-1} \int_0^\infty \kappa^{-(\beta-1)} \left[1 - \frac{4J_1^{\,2}(\kappa)}{\kappa^2} \right] \mathrm{d}\kappa \right\} . \tag{A10}$$

This normalization ensures that the sum of the Zernike-coefficient variances from $j = 2$ to infinity sum to unity, consistent with Eq. (8). Following Noll,[14] we have for the integral in Eq. (A10)

$$\begin{aligned} &\int_0^\infty \kappa^{-(\beta-1)} \left\{ 1 - \frac{4J_1^{\,2}(\kappa)}{\kappa^2} \right\} \mathrm{d}\kappa \\ &= \frac{\pi \Gamma(\beta+1)}{2^{\beta-1} \left[\Gamma\left(\frac{\beta+2}{2} \right) \right]^2 \Gamma\left(\frac{\beta+4}{2} \right) \Gamma\left(\frac{\beta}{2} \right) \sin\left(\pi \frac{\beta-2}{2} \right)} , \end{aligned} \tag{A11}$$

valid over the range $2 < \beta < 4$. We thus have for A_β,

$$\begin{aligned} A_\beta &= \frac{1}{2\pi^{\beta-1} \dfrac{\pi \Gamma(\beta+1)}{2^{\beta-1} \left[\Gamma\left(\frac{\beta+2}{2} \right) \right]^2 \Gamma\left(\frac{\beta+4}{2} \right) \Gamma\left(\frac{\beta}{2} \right) \sin\left(\pi \frac{\beta-2}{2} \right)}} , \end{aligned} \tag{A12}$$

$$A_\beta = \frac{2^{\beta-2} \left[\Gamma\left(\frac{\beta+2}{2} \right) \right]^2 \Gamma\left(\frac{\beta+4}{2} \right) \Gamma\left(\frac{\beta}{2} \right) \sin\left(\pi \frac{\beta-2}{2} \right)}{\pi^\beta \Gamma(\beta+1)} . \tag{A13}$$

ACKNOWLEDGMENTS

This work was supported in part by the United Kingdom Particle Physics and Astronomy Research Council under grant GR/H 64156 and by a sabbatical from the University of Central Florida. We thank Geoff Stephenson of the Mathematics Department of Imperial College for helpful discussions.

REFERENCES

1. V. I. Tatarski, *Wave Propagation in a Turbulent Medium* (McGraw Hill, New York, 1961), Chap. 2.
2. D. L. Fried, "Statistics of a geometric representation of wave-front distortion," J. Opt. Soc. Am. **55,** 1427–1435 (1965).
3. D. L. Fried, "Optical resolution through a randomly inhomogeneous medium for very long and very short exposures," J. Opt. Soc. Am. **56,** 1372–1379 (1966).
4. F. Dalaudier, A. S. Gurvich, V. Kan, and C. Sidi, "Middle stratosphere temperature spectra observed with stellar scintillation and *in situ* techniques," Adv. Space Res. **14,** 61–64 (1994).
5. M. S. Belen'kii and A. S. Gurvich, "Influence of the stratospheric turbulence on infrared imaging," in *Atmospheric Propagation and Remote Sensing IV,* J. C. Dainty, ed., Proc. Soc. Photo-Opt. Instrum. Eng. **2471,** 260–271 (1995).
6. R. G. Buser, "Interferometric determination of the distance dependence of the phase structure function for near-ground horizontal propagation at 6326 Å," J. Opt. Soc. Am. **61,** 488–491 (1971).
7. M. Bester, W. C. Danchi, C. G. Degiacomi, L. J. Greenhill, and C. H. Townes, "Atmospheric fluctuations—empirical structure functions and projected performance of future instruments," Astrophys. J. **392,** 357–374 (1992).
8. D. Dayton, B. Pierson, B. Spielbusch, and J. Gonglewski, "Atmospheric structure function measurements with a

Shack–Hartmann wave-front sensor," Opt. Lett. **17,** 1737–1739 (1992).
9. A. I. Kon, "Qualitative theory of amplitude and phase fluctuations in a medium with anisotropic turbulent irregularities," Waves Random Media **4,** 297–306 (1994).
10. B. E. Stribling, B. M. Welsh, and M. C. Roggemann, "Optical propagation in non-Kolmogorov atmospheric turbulence," in *Atmospheric Propagation and Remote Sensing IV,* J. C. Dainty, ed., Proc. Soc. Photo-Opt. Instrum. Eng. **2471,** 181–196 (1995).
11. B. E. Stribling, "Laser beam propagation in non-Kolmogorov atmospheric turbulence," M. S. thesis (Air Force Institute of Technology, Wright-Patterson Air Force Base, Ohio, 1994).
12. D. M. Winker, "Effect of a finite outer scale on the Zernike decomposition of atmospheric optical turbulence," J. Opt. Soc. Am. A **8,** 1568–1573 (1991).
13. T. W. Nicholls, G. D. Boreman, and J. C. Dainty, "Use of a Shack–Hartmann wave-front sensor to measure deviations from a Kolmogorov phase spectrum," Opt. Lett. **20,** 2460–2462 (1995).
14. R. J. Noll, "Zernike polynomials and atmospheric turbulence," J. Opt. Soc. Am. **66,** 207–211 (1976).
15. J. Y. Wang and J. K. Markey, "Modal compensation of atmospheric turbulence phase distortion," J. Opt. Soc. Am. **68,** 78–87 (1978).
16. I. S. Gradshteyn and I. M. Ryzhik, *Table of Integrals, Series, and Products,* 5th ed. (Academic, New York, 1994), formula 6.574.2.
17. V. V. Voitsekhovich, "Outer scale of turbulence: comparison of different models," J. Opt. Soc. Am. A **12,** 1346–1353 (1995).